

# Do Nudging Tendencies Depend on the Nudging Timescale Chosen in Atmospheric Models?

Kruse Christopher G<sup>1</sup>, Bacmeister Julio T.<sup>2</sup>, Zarzycki Colin M.<sup>3</sup>, Larson Vincent E<sup>4</sup>, and Thayer-Calder Katherine<sup>2</sup>

<sup>1</sup>NorthWest Research Associates

<sup>2</sup>National Center for Atmospheric Research (UCAR)

<sup>3</sup>Pennsylvania State University

<sup>4</sup>University of Wisconsin-Milwaukee

November 16, 2022

## Abstract

Nudging is a ubiquitous capability of numerical weather and climate models that is widely used in a variety of applications (e.g. crude data assimilation, “intelligent” interpolation between analysis times, constraining flow in tracer advection/diffusion simulations). Here, the focus is on the momentum nudging tendencies themselves, rather than the atmospheric state that results from application of the method.

The initial intent was to interpret these tendencies as a quantitative estimation of model error (net parameterization error in particular). However, it was found that nudging tendencies depend strongly on the nudging time scale chosen, which is the primary result presented here. Reducing the nudging time scale reduces the difference between the model state and the target state, but much less so than the reduction in the nudging time scale, resulting in increased nudging tendencies. The dynamical core, in particular, appears to increasingly oppose nudging tendencies as the nudging time scale is reduced. These results suggest nudging tendencies cannot be *quantitatively* interpreted as model error. Still, nudging tendencies do contain some information on model errors and/or missing physical processes and still might be useful in model development and tuning, even if only qualitatively.

# Do Nudging Tendencies Depend on the Nudging Timescale Chosen in Atmospheric Models?

<sup>1,2</sup>Christopher G. Kruse, <sup>1</sup>Julio T. Bacmeister, <sup>3</sup>Colin M. Zarzycki, <sup>4,5</sup>Vincent E. Larson, and <sup>1</sup>Katherine Thayer-Calder

<sup>1</sup>National Center for Atmospheric Research, Climate and Global Dynamics Laboratory, Boulder, Colorado

<sup>2</sup>NorthWest Research Associates, Boulder, Colorado

<sup>3</sup>Pennsylvania State University, Department of Meteorology and Atmospheric Science, University Park, Pennsylvania

<sup>4</sup>University of Wisconsin - Milwaukee, Department of Mathematical Sciences, Milwaukee, Wisconsin

<sup>5</sup>Pacific Northwest National Laboratory, Richland, Washington

## Key Points:

- Nudging tendencies, or nudging forces per unit mass, depend strongly on the nudging time scale chosen (i.e. are  $\propto \tau_{ndg}^{-1}$ ).
- Nudging tendencies cannot be *quantitatively* interpreted as errors in total (dynamics + physics) model forces on the atmospheric fluid
- Still, time-averaged differences between the modeled and target states can be useful in metrics for model evaluation.

---

Corresponding author: Christopher G. Kruse, [ckruse@nwra.com](mailto:ckruse@nwra.com)

## Abstract

Nudging is a ubiquitous capability of numerical weather and climate models that is widely used in a variety of applications (e.g. crude data assimilation, “intelligent” interpolation between analysis times, constraining flow in tracer advection/diffusion simulations). Here, the focus is on the momentum nudging tendencies themselves, rather than the atmospheric state that results from application of the method. The initial intent was to interpret these tendencies as a quantitative estimation of model error (net parameterization error in particular). However, it was found that nudging tendencies depend strongly on the nudging time scale chosen, which is the primary result presented here. Reducing the nudging time scale reduces the difference between the model state and the target state, but much less so than the reduction in the nudging time scale, resulting in increased nudging tendencies. The dynamical core, in particular, appears to increasingly oppose nudging tendencies as the nudging time scale is reduced. These results suggest nudging tendencies cannot be *quantitatively* interpreted as model error. Still, nudging tendencies do contain some information on model errors and/or missing physical processes and still might be useful in model development and tuning, even if only qualitatively.

## Plain Language Summary

Nudging is a common feature of weather and climate models used to guide the model’s atmospheric state along the observed atmospheric evolution in the past. Here, an initial attempt was made to interpret the nudging tendencies as model error. However, it was learned that these nudging tendencies change when the nudging time scale is changed, largely due to the model’s dynamical core opposing the effect of the nudging in trying to achieve its desired state. Results presented here suggest the model wins this “tug-of-war.” The overall conclusion is that these nudging tendencies cannot be quantitatively interpreted as model error, but still have some use in identifying model issues, even if only qualitatively.

## 1 Introduction

Nudging atmospheric models is a process where a linear relaxation term is introduced into the governing equation for some variable (e.g. the zonal wind,  $u$ ). The nudging term produces a tendency that acts to bring that variable toward some target state. For example, the prognostic equation for  $u$  can be written

$$\frac{\partial u}{\partial t} = D_x(\boldsymbol{\phi}) + P_x(\boldsymbol{\phi}) + N_x(u, u_0), \quad (1)$$

where  $D_x(\cdot)$  is the sum of zonal wind tendencies from dynamical terms (e.g. advection, pressure gradient, Coriolis),  $P_x(\cdot)$  is the sum of zonal wind tendencies from physical parameterizations (turbulence, gravity wave drag, ...),  $\boldsymbol{\phi}$  a vector of variables making up the state required by dynamics and physics model components, and  $N_x(u, u_0)$  is the added linear relaxation nudging term defined below.

The form of nudging term,  $N_x(u, u_0)$ , depends on the type of target state,  $u_0$ . For example, the target state might be a particular observation, with nudging tendencies proportional to the difference between the model state and the observation, inversely proportional to distance in space and time, and inversely proportional to some specified nudging time scale,  $\tau_{ndg}$ . This approach is referred to as observational nudging. Another possibility is that the target state is a gridded analysis, referred to as analysis nudging. In this case, the nudging term often takes the following form:

$$N_x(u, u_0) = -W \left( \frac{u - u_0}{\tau_{ndg}} \right) \quad (2)$$

where  $u_0 = u_0(x, y, z, t)$  is some target state (e.g. analysis) spatiotemporally interpolated onto the host model grid and  $W = W(x, y, z, t)$  is a weighting function that can be used to limit nudging to certain regions, model levels, or times. Here, analysis nudging is the focus with the weighting function set to unity ( $W = 1$ ).

The use of such nudging first appears in scientific literature in the mid-1970s (Kistler, 1974; Anthes, 1974; Davies & Turner, 1977). The original application was to use nudging to assimilate data for analyses and model initial conditions. This approach more continuously assimilated information from data, preventing numerical instabilities that arose in previous assimilation methods that simply inserted observations (e.g. Charney et al. (1969); Jastrow and Halem (1970)). For additional early historical context and applications, see Stauffer and Seaman (1990) and Skamarock et al. (2008).

Subsequently, another application of analysis nudging was first demonstrated in Kao and Yamada (1988), where a numerical weather model was nudged to analyzed observations, allowing realistic tracer transport and diffusion with synoptic-scale meteorology constrained. Such an exercise was sometimes preferable to just using the standard 12-hourly analyses of the time, allowing physical processes represented in the model to influence the state trajectory and tracer advection/diffusion between analyses in a plausible way. Currently, using analysis nudging to constrain meteorology in advection, diffusion, and chemistry models is fairly common, often referred to as a “specified dynamics” configuration of some host model (e.g. Davis et al. (2021)).

Here, the initial intent was to use nudging to approximate errors in model parameterizations, with particular interest in errors in the momentum equations. As nudging keeps the host model’s state close to a presumably accurate target state, one might interpret the nudging tendencies time averaged over, say, a season, to be the net error in total (i.e. dynamical core + all parameterization tendencies) model forcing per unit mass (Eq. 1). If one were to further assume dynamical core errors are significantly smaller than those introduced by the physical parameterizations and the target state is accurate, then the nudging tendencies might be interpreted more specifically as the net error of all parameterizations. Then, nudging tendencies and physical understanding of relevant processes at play could be used to attribute errors to particular processes and these errors might be quantitatively targeted. Mapes and Bacmeister (2012) use similar arguments to interpret incremental analysis update tendencies as net error of all physics parameterizations.

However, while evaluating such an approach, it was found that nudging tendencies are proportional to the inverse of the nudging time scale ( $\tau_{ndg}^{-1}$ ) chosen and, therefore, cannot be interpreted as total model (dynamics + physics) error or net physics error, at least not *quantitatively*. The sole objective of this article is to present this apparently unpublished, if not completely unknown, result. The ubiquity of nudging capabilities and their many, frequent uses within weather and climate models motivate presentation of this result.

Here, nudging tendencies required to keep the Community Atmosphere Model, version 6 (CAM6, Gettelman et al. (2019)), close to the ERA5 reanalysis (Hersbach et al., 2020) over five recent winters are analyzed, with nudging time scales varied from 3 to 24 hours. The model configuration and experiments are described in Section 2. The primary result that nudging tendencies are proportional to  $\tau_{ndg}^{-1}$  is presented in Section 3. In Section 4, a heuristic theoretical argument for this result is provided. A summary and discussion of the results is given in Section 5.

## 2 Model Configuration and Experiment Design

The default CAM6 was used to simulate five winters from 2008 to 2012 with specified sea surface temperatures and sea ice (i.e. the “FHIST” component set was specified) on a  $\approx 1$  degree latitude/longitude grid with the finite-volume dynamical core. The model was initialized every 1 Dec with ERA5 interpolated onto its grid and integrated for three months (i.e. over December, January, and February (DJF)). During the integrations, CAM was continuously nudged to ERA5 winds, temperatures, and humidities at every time step. With a time step of 30 minutes, the target state,  $\phi_0 = (u_0, v_0, T_0, q_0)$ , was updated to ERA5 at the top of every hour and to ERA5 linearly interpolated in time half-past every hour. Four such simulations of these five winters were completed, each with a constant nudging time scale of  $\tau_{ndg} = 3, 6, 12,$  and 24 hours.

All tendencies acting on the zonal and meridional winds were output. Exact budget closure was verified. Here, generally, the net tendencies by the dynamical core and by all physical parameterizations are presented, often referred to as “dynamics” and “physics” tendencies. Figure 1 shows the DJF-averaged net dynamics, physics, and nudging tendencies projected along the DJF-averaged wind horizontal wind vector vertically averaged over the lowest four levels. For example, the nudging tendencies in Fig. 1d were computed via

$$\overline{N} = \frac{\int \langle \mathbf{N} \rangle \cdot \langle \widehat{\mathbf{u}} \rangle \langle \rho \rangle dz}{\int \langle \rho \rangle dz}. \quad (3)$$

where  $\langle . \rangle$  is a DJF, 2008-2012 time average and  $\langle \widehat{\mathbf{u}} \rangle$  is a unit vector pointing in the direction of the DJF, 2008-2012 time averaged horizontal wind vectors.

### 2.1 Typical DJF Momentum Balances

Here, the focus is on the lowest four model levels, as an initial interest was low-level wind biases that nudging tendencies at these levels highlight. Generally, the dynamical core acts to accelerate the low-level flow (Fig. 1a), while the physical parameterizations (the turbulence and low-level drag parameterizations in particular) oppose these dynamics tendencies and act to decelerate the low-level flow (Fig. 1b). The dynamics and physics tendencies do not exactly cancel, however (Fig. 1c). The residual of these two tendencies is almost exactly compensated by the nudging tendencies. This is expected, as  $\partial_t \mathbf{u} \approx \mathbf{0}$  after time averaging over DJF, requiring the sum of the dynamics/physics residual tendencies and the nudging tendencies to be small as well (Eq. 1). The total wind time-averaged tendencies are an order of magnitude smaller than those in the bottom row of Fig. 1 (not shown).

## 3 Do Nudging Tendencies Change with $\tau_n$ ?

To get a sense for how robust nudging-tendency-derived model error estimates were, nudging time scales were varied while keeping the model configuration (default except for the nudging) unchanged. The momentum nudging tendencies,  $\overline{N}$ , are shown in Fig. 2 for four runs with  $\tau_{ndg}$  varied from 3 to 24 hours.

Two results are immediately apparent: the spatial structure of the momentum nudging tendencies are quite consistent across the four runs and the nudging tendencies increase with decreasing  $\tau_{ndg}$ . These results held when looking at the middle troposphere and lower stratosphere as well (not shown). Nudging tendencies tend to exert additional drag over regions with significant topography (e.g. the Andes, the Rocky Mountains, the Himalayas, the flanks of Antarctica) in all four simulations. These tendencies also exert drag on the low-level winds in all four runs over the Southern Ocean, with tenden-

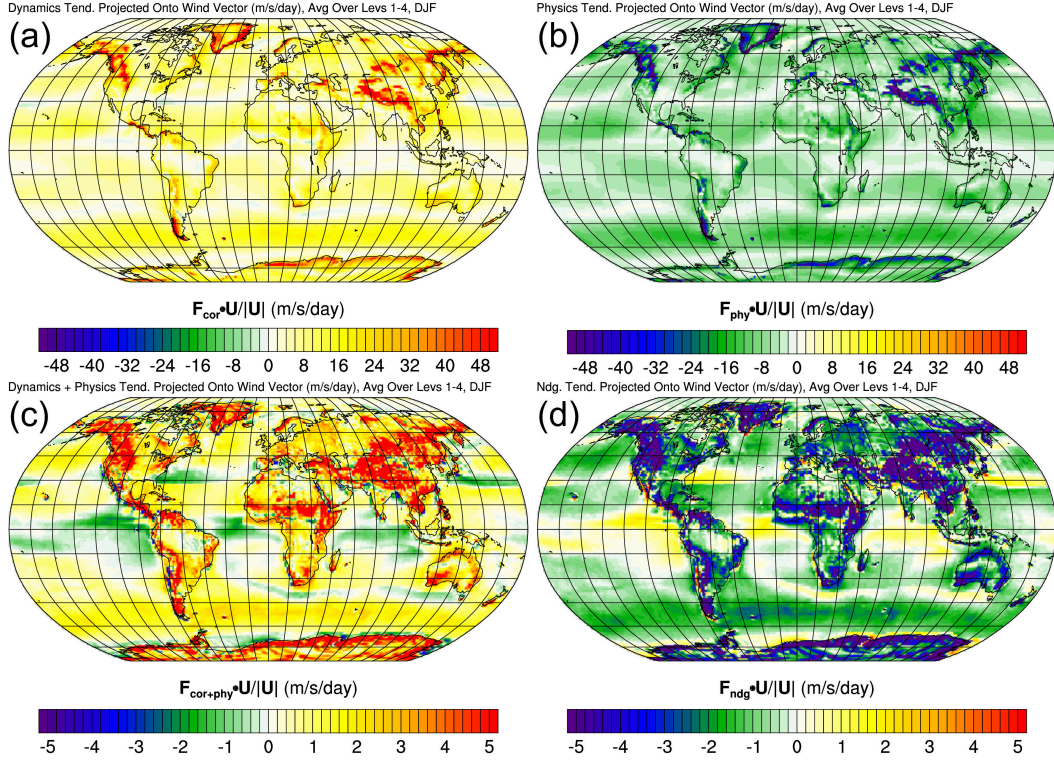


**Figure 1.** DJF-, 2008-2012-averaged horizontal momentum budget components projected along the similarly averaged horizontal wind and vertically averaged over the lowest four model levels, computed via Eq. 3, are color shaded. The net dynamics tendencies ( $\overline{D}$ ) and net physics tendencies ( $\overline{P}$ ) are shown in (a) and (b). The sum of dynamics and physics ( $\overline{D} + \overline{P}$ ) are shown in (c). Nudging tendencies ( $\overline{N}$ ) are shown in (d). Note the different order of magnitude in the color bars in each row.

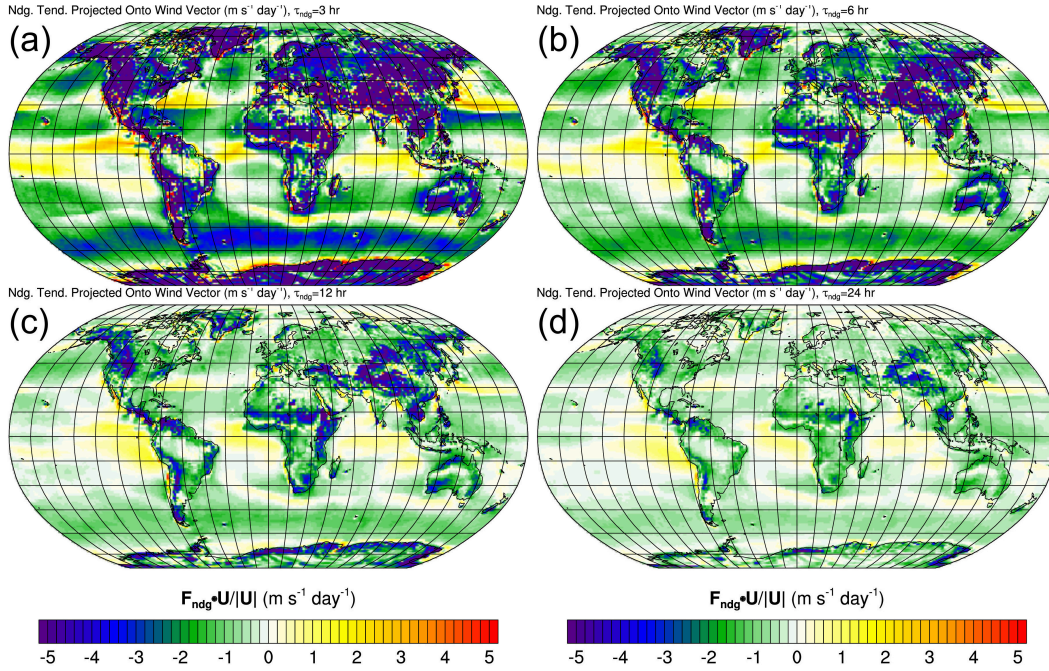


**Figure 2.** DJF-, 2008-2012-averaged horizontal momentum nudging tendencies projected along the similarly averaged horizontal wind and vertically averaged over the lowest four model levels are color shaded. The four panels show maps of these nudging tendencies from four runs with nudging time scales of (a) 3 hours, (b) 6 hours, (c) 12 hours, and (d) 24 hours.

152 cies somewhat invariant in longitude at these latitudes. Regions where the model might  
 153 be exerting too much drag and the nudging tendencies tend to accelerate the low-level  
 154 flow also display some consistency across the runs, though, perhaps less so than the re-  
 155 gions of inferred too little drag.

156 Scatter plots of time-averaged zonal dynamics, physics, and momentum nudging  
 157 tendencies at individual grid points on the lowest four model levels from one run plot-  
 158 ted versus corresponding tendencies from the run with twice the nudging time scale are  
 159 shown in Fig. 3. Best fit linear regressions and  $r^2$  values shown in each panel. Nudging  
 160 tendencies at individual grid points are consistent between runs with  $\tau_{ndg}$  changed by  
 161 a factor of two, indicated by the fairly linear relation between the nudging tendencies  
 162 and the high  $r^2$  ( $\geq 0.911$ ) values. Slopes of the linear regressions are significantly larger  
 163 than one, though, a bit less than the expected slope of 2 if nudging tendencies were ex-  
 164 actly proportional to the inverse nudging time scale. However, these regressions are in-  
 165 fluenced by a majority of points with small tendencies. Grid points with the largest ten-  
 166 dencies do track more closely to a 2-to-1 line. Regardless, the nudging tendencies are roughly  
 167 proportional to  $\tau_{ndg}^{-1}$  over  $\tau_{ndg}$  ranging from 3 to 24 hours even grid-point by grid-point.  
 168 The dynamics and physics tendencies are much more consistent when  $\tau_{ndg}$  is changed  
 169 by a factor of 2, falling much closer to a 1-to-1 line.

170 Similar maps and scatter plots of temperature nudging tendencies are shown in Figs. 4  
 171 and 5. Temperature nudging tendencies have a similar dependence on  $\tau_{ndg}$ , with ten-  
 172 dencies also increasing with decreasing  $\tau_{ndg}$ . However, this dependence is less strong than  
 173 that with the momentum nudging tendencies (c.f. Figs. 3 and 5 a-c).

174 If nudging tendencies were to give a robust/consistent estimate of model error of  
 175 a model in a particular configuration, one might expect that the difference between the

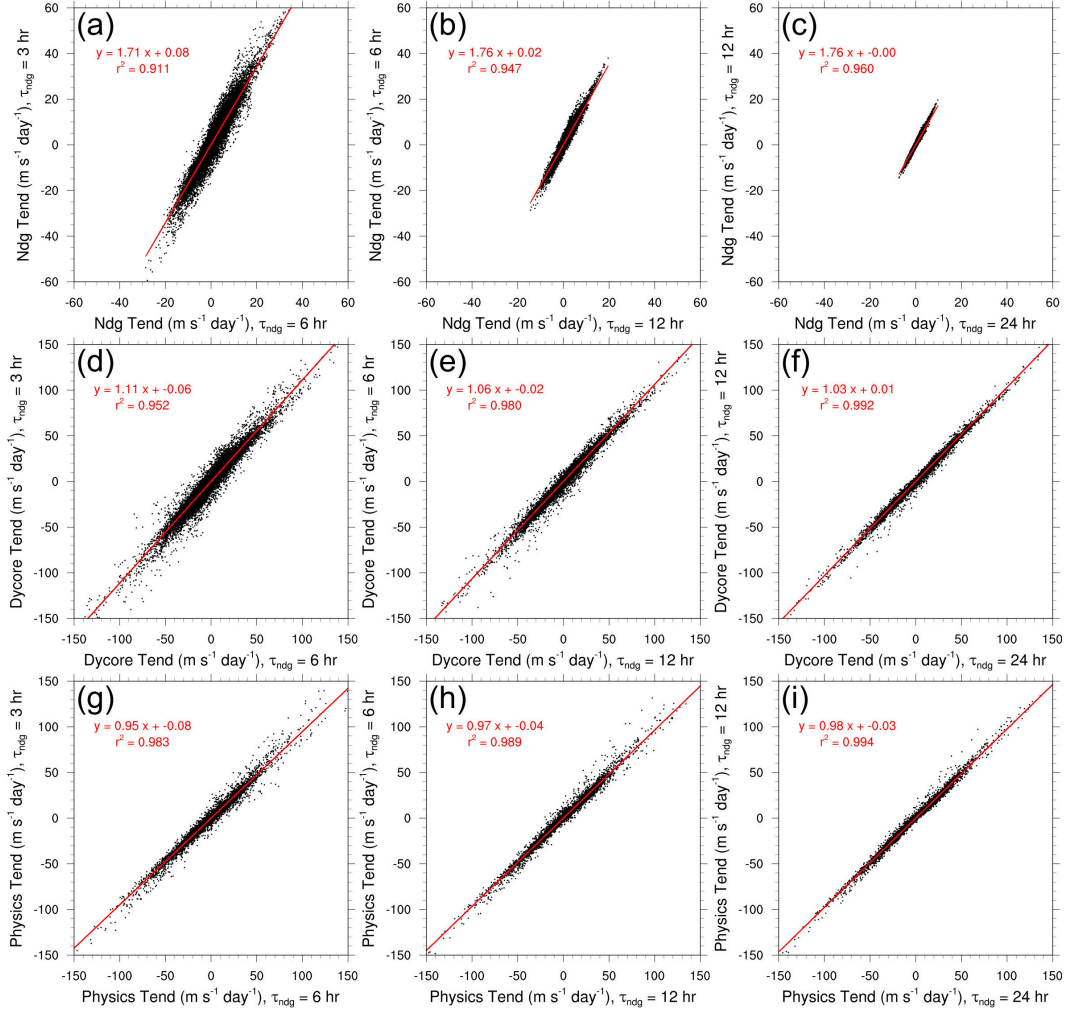


**Figure 3.** Scatter plots of (top) nudging, (middle) dynamical core, and (bottom) physics tendencies from a nudging run plotted versus the same quantities from a run with twice the nudging time scale. Each point represents the DJF, 5-season time averaged tendency on a grid point on one of the four lowest model levels. Runs with nudging time scales of 3, 6, 12, and 24 hours were used. Best fit lines and corresponding  $r^2$  values are overlaid in red.

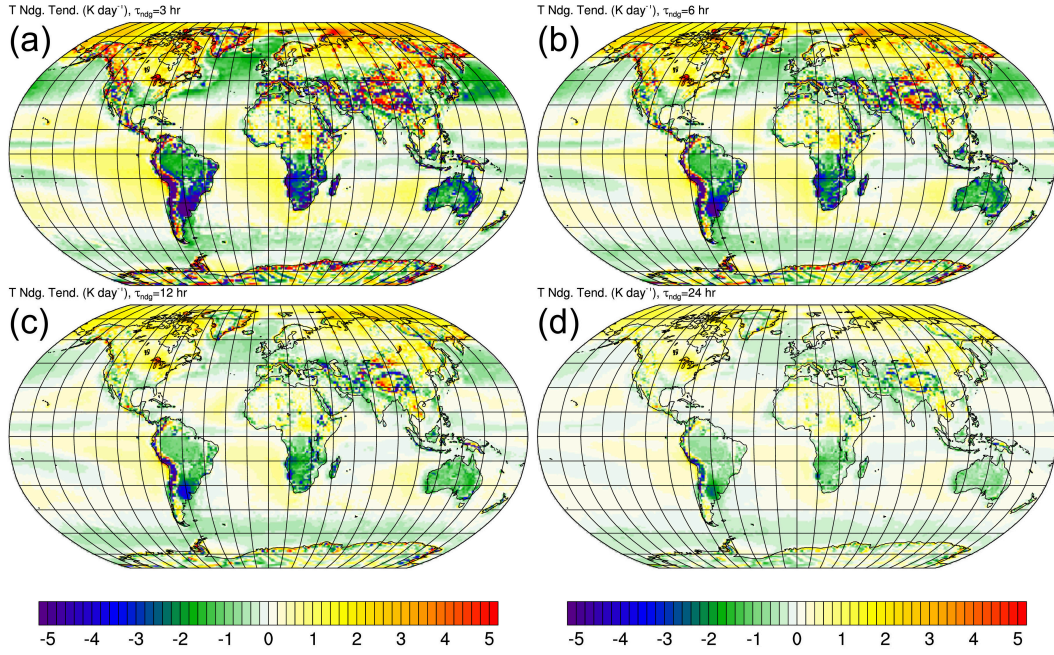


**Figure 4.** DJF-, 2008-2012-averaged temperature nudging tendencies vertically averaged over the lowest four model levels are shown in color shading. The four panels show maps of these nudging tendencies from four runs with nudging time scales of (a) 3 hours, (b) 6 hours, (c) 12 hours, and (d) 24 hours.

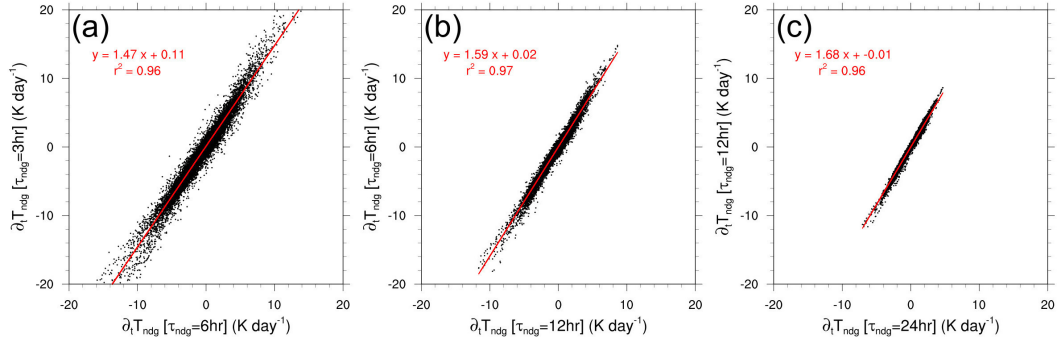


**Figure 5.** Scatter plots of temperature nudging tendencies from a nudging run plotted versus the same quantities from a run with twice the nudging time scale. Each point represents the DJF, 5-season time averaged tendency on a grid point on one of the four lowest model levels. Runs with nudging time scales of 3, 6, 12, and 24 hours were used. Best fit lines and corresponding  $r^2$  values are overlaid in red.

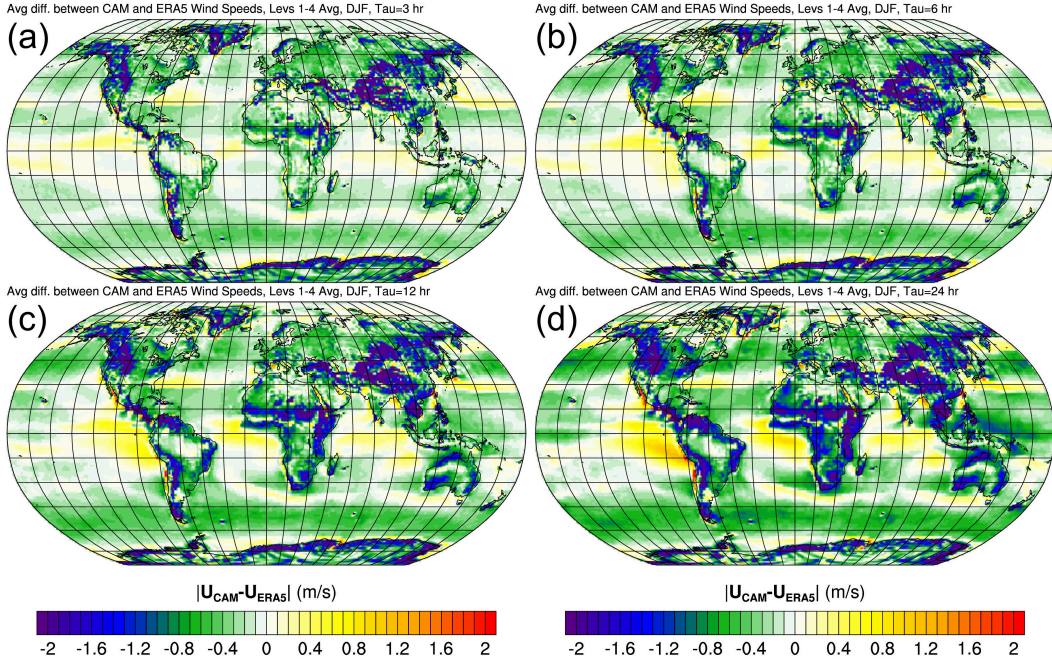


**Figure 6.** Same as Fig. 2, but with each panel multiplied by its corresponding nudging time scale. This gives the time-average, level-1-4-average, difference in wind speed between CAM and ERA5.

	3 hr vs 6 hr	6 hr vs 12 hr	12 hr vs 24 hr
Slope	0.87	0.89	0.89
Offset	0.01	0.01	0.00
$r^2$	0.92	0.95	0.96

**Table 1.** Linear regression coefficients and  $r^2$  values from scatter plots of  $\tau_{ndg,1}(\mathbf{N}) \cdot \widehat{\langle \mathbf{u} \rangle}$  plotted vs  $\tau_{ndg,2}(\mathbf{N}) \cdot \widehat{\langle \mathbf{u} \rangle}$ , where  $\tau_{ndg,1} = 0.5\tau_{ndg,2}$ . These differences on the lowest four model levels were used, without the vertical averaging applied in Fig. 6, Eq. 3. Scatter plots not shown.

176 model state and the target state (i.e. the numerator in Eq. 2) to reduce proportionately  
 177 to the reduction in nudging time scale. Given that nudging tendencies increase, the dif-  
 178 ference between the model state and the target state is not being reduced proportion-  
 179 ately. The DJF-2008-2012-, level-1-4-averaged momentum nudging tendencies,  $\overline{\mathbf{N}}$ , in Fig. 2  
 180 are multiplied by the  $\tau_{ndg}$  used in each run to illustrate how the time-averaged differ-  
 181 ence between the model and target state varies in Fig. 6. Decreasing the nudging time  
 182 scale by a 50% does bring the model state closer to the target state, but only by  $\approx 12\%$   
 183 (Table 1).

184 Because nudging does keep the model state close to the target state (Fig. 6) and  
 185 the DJF-2008-2012-average total wind tendencies are an order of magnitude smaller than  
 186 the nudging tendencies in all runs ( $\partial_t \mathbf{u} \approx 0$ , not shown), the momentum budget (e.g.  
 187 Eq. 1) requires a compensation in model tendencies somewhere. This is hinted at by the  
 188 anti-correlation of the net model tendencies and nudging tendencies in the bottom row  
 189 of Fig. 1, consistent with Bao and Errico (1997) (their Section 4). The changes in dy-  
 190 namics and physics tendencies are plotted versus the changes in nudging tendencies on  
 191 grid points in Fig. 7 for runs with  $\tau_{ndg}$  changed by a factor of two. Interestingly, this com-

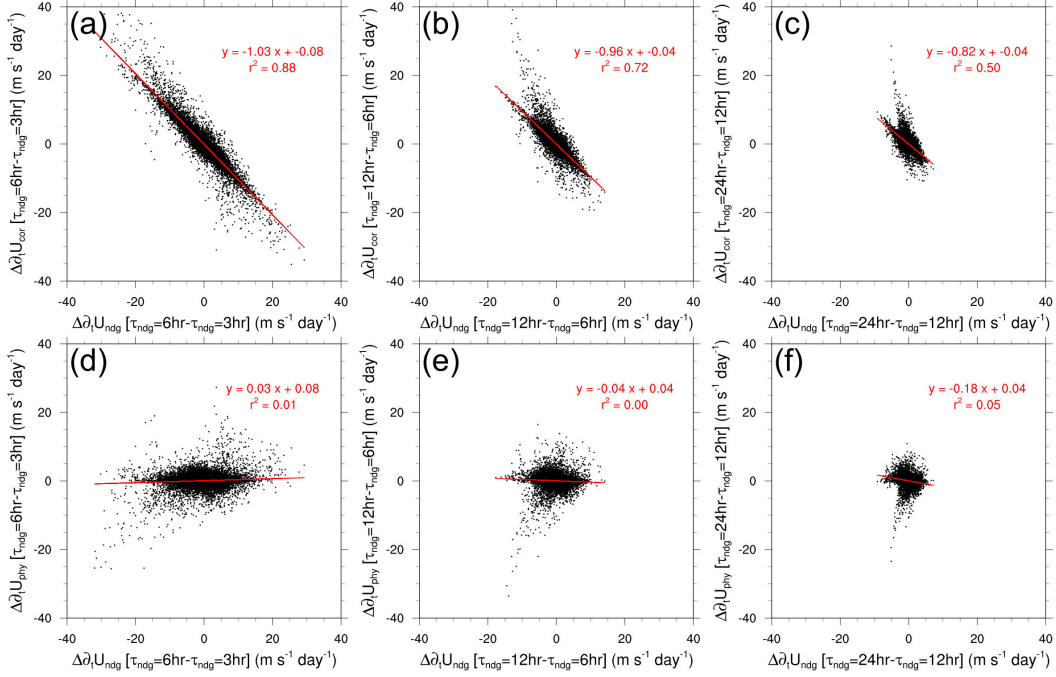


**Figure 7.** Scatter plots of changes of (top) dynamical core tendencies and (bottom) physics tendencies plotted versus changes in nudging tendencies when reducing nudging time scales by a factor of two. Each point represents such differences in DJF, 5-season averaged tendencies at grids points on one of the lowest four model levels.

192      pensation occurs primarily in dynamics tendencies, being particularly clear at the smaller  
193      nudging time scales.

194      These results suggest that, at least when the model configuration is not changed,  
195      the physical processes represented by the dynamical core are primarily responsible for  
196      compensating these nudging tendencies. In other words, the dynamical core is respon-  
197      sible for fighting the effect of the nudging and reducing the ability of the nudging term  
198      to bring the model state closer to the target state. A heuristic theoretical representa-  
199      tion of the nudged model system is presented in the following section to speculate on how  
200      the dynamical core is fighting the nudging tendencies and why these tendencies are pro-  
201      portional to the inverse nudging time scale.

#### 202      4 Time Scale Analysis

203      Some progress can be made in understanding why nudging tendencies vary with  
204       $\tau^{-1}$  using a simple time scale analysis. Here, the entire host model (i.e.  $D_x(\phi) + P_x(\phi)$ )  
205      is heuristically represented by a linear relaxation term:

$$\frac{\partial u}{\partial t} \approx -\frac{u - u_{mod}}{\tau_{mod}} - \frac{u - u_0}{\tau_{ndg}} \quad (4)$$

206      where  $u_{mod}$  is some zonal wind the model is trying to achieve on some model timescale,  
207       $\tau_{mod}$ . A target state for the whole nudged system ( $u_s$ ) and system relaxation time scale  
208      ( $\tau_s$ ) are defined as

$$\tau_s = \frac{\tau_{ndg}\tau_{mod}}{\tau_{ndg} + \tau_{mod}}, \quad (5)$$

209 and

$$\frac{u_s}{\tau_s} = \frac{u_{mod}}{\tau_{mod}} + \frac{u_0}{\tau_{ndg}}. \quad (6)$$

210 With these definitions, the state of the nudged model system can be expressed as a weighted  
211 average of the nudging and model time scales:

$$u_s = \frac{\tau_{ndg}}{\tau_{ndg} + \tau_{mod}}u_{mod} + \frac{\tau_{mod}}{\tau_{ndg} + \tau_{mod}}u_0. \quad (7)$$

Correspondingly, the momentum equation can be written as

$$\frac{\partial u}{\partial t} \approx -\frac{u - u_s}{\tau_s}. \quad (8)$$

212 In this simple system, the model is trying to achieve its desired state (i.e. the model is  
213 pulling the nudged system state toward its attractor,  $u_{mod}(x, y, z, t)$ ) while the nudging  
214 term is trying to pull the nudged model's state to the target state ( $u_0(x, y, z, t)$ , Eq. 4).  
215 Alternatively, the nudged model state is essentially being relaxed to a timescale-weighted  
216 average of the target and model attractor states on the system timescale (Eq. 8).

217 Eq. 8 implies that, averaged over sufficient time, the time-averaged nudged model  
218 state should just be the time-averaged system state:

$$\langle u \rangle^t = \langle u_s \rangle^t. \quad (9)$$

219 where  $\langle \cdot \rangle^t$  is a time-average operator. The time-averaged nudging tendencies were pre-  
220 sented in the previous section. The following expression for the time-averaged nudging  
221 tendencies follows from Eqs. 2, 7, and 9:

$$\langle N_x \rangle^t = -\frac{\langle u \rangle^t - \langle u_0 \rangle^t}{\tau_{ndg}} = -\frac{\langle u_{mod} \rangle^t - \langle u_0 \rangle^t}{\tau_{mod} + \tau_{ndg}} \quad (10)$$

222 This relation suggests that as long as the state the host model is trying to achieve (i.e.  
223 its attractor,  $\langle u_{mod} \rangle^t$ ) differs from the target state ( $\langle u_0 \rangle^t$ ) systematically, there will be  
224 non-zero time-averaged nudging tendencies. The magnitude of these nudging tendencies  
225 depends on how different the state the host model is trying to achieve and the target state  
226 are. The model and nudging time scales also play a role. However, if the model time scale  
227 is sufficiently small relative to the nudging time scale ( $\tau_{mod} \ll \tau_{ndg}$ ), or it is some-  
228 how dictated by the imposed nudging time scale (i.e.  $\tau_{mod} \propto \tau_{ndg}$ ), then the time av-  
229 eraged nudging tendencies will be proportional to the inverse of the nudging time scale,  
230 consistent with the model result presented above. The model time scale is further dis-  
231 cussed and estimated from the model output below.

#### 232 4.1 Model Time Scales

233 What is this model time scale and what values might it have? Nudging tendencies  
234 likely act to bring the model away from its desired state, while the model (i.e. the dy-  
235 namical core in particular) tends to oppose these tendencies as it tries to achieve its de-  
236 sired state. Here, it is speculated that the model relaxation term in Eq. 4 represents the  
237 host model's adjustment to imbalances produced by dynamical, physical or nudging ten-  
238 dencies. A classical, albeit idealized, example of a fluid adjusting from an imbalanced  
239 state to a balanced one is geostrophic adjustment (Blumen, 1972). In the geostrophic

240 adjustment problem, the time scale of adjustment is usually treated as an order of mag-  
 241 nitude smaller than the time scale of evolution of a fluid in geostrophic balance. In ab-  
 242 solute terms, geostrophic adjustment occurs over a time scale of an inertial period ( $2\pi/f$ ,  
 243 where  $f$  is the Coriolis parameter), which depends on latitude, but has values of 12 hours  
 244 at the poles that increase toward the equator. In reality, and within numerical models,  
 245 excess momentum associated with a variety of physical imbalances (e.g. deviations from  
 246 cyclo-geostrophic balance, quasi-geostrophic balance, semi-geostrophic balance, non-linear  
 247 balance) is shed via generation of, and transport by, atmospheric waves (e.g. gravity waves  
 248 (GWs), inertia gravity waves, Kelvin waves, (Plougonven & Zhang, 2014)). Outside of  
 249 the tropics, GWs are emitted from these imbalances, having time scales ranging from  
 250 the buoyancy period ( $\approx 10$  minutes) to the inertial period ( $\approx 10$  hours). If the time  
 251 scale of adjustment to the imbalances produced by the nudging tendencies is similar to  
 252 the time scales of the waves generated by the adjustment process, then  $\tau_{mod}$  would likely  
 253 be in the range of 10 minutes to 10 hours. This range of  $\tau_{mod}$  ( $10 \text{ min} \lesssim \tau_{mod} \lesssim 10 \text{ hrs}$ )  
 254 is a bit smaller than the range of  $\tau_{ndg}$  ( $3 \text{ hrs} \leq \tau_{ndg} \leq 24 \text{ hrs}$ ) used here, and so might  
 255 be consistent with argument above that nudging tendencies are proportional to  $\tau_{ndg}^{-1}$  be-  
 256 cause  $\tau_{mod} \ll \tau_{ndg}$ .

257 Here, the model relaxation time scales were estimated from the 3-hourly-averaged  
 258 momentum tendencies by regressing the model tendencies (i.e.  $D_x + P_x$ ) versus the dif-  
 259 ference between the 3-hourly-averaged nudged-system and model attractor states,  $u -$   
 260  $u_{mod}$ . This difference is not known because  $u_{mod}$  is not known. However, if the differ-  
 261 ences between the time-varying target state and the model's desired state are much smaller  
 262 than the time-varying differences of the nudged model system state from the model's de-  
 263 sired state or the target state,

$$|(u - u_{mod}) - (u - u_0)| = |u_0 - u_{mod}| \ll |u - u_{mod}|, |u - u_0|,$$

264 then  $u - u_{mod}$  can be approximated by  $u - u_0$ , which can be easily computed from the  
 265 nudging tendencies multiplied by the corresponding  $\tau_{ndg}$ . The model tendencies were re-  
 266 gressed against  $u - u_0$  at every grid point on the 4th model level, and the model time  
 267 scales were then computed from the inverse of the regression slopes. These estimates of  
 268  $\tau_{mod}$  are shown in Fig. 8 in both absolute units and relative to the nudging time scale  
 269 used. Regions color shaded are those where the probability the regression slope is non-  
 270 zero is greater than 99%. An additional consistency check on this approach is provided  
 271 by the correlation coefficients between  $D_x + P_x$  and  $u - u_{mod}$  (not shown). Correla-  
 272 tions are modest but generally significant, with values in the range of -0.5 to -0.75 in parts  
 273 of the Southern Ocean and Subtropics.

274 The magnitude of the  $\tau_{mod}$  estimate is quite variable across the globe (left column  
 275 of Fig. 8). This might not be so surprising, as time scales of geostrophic adjustment and  
 276 maximum time scales of GWs that can be emitted both decrease with increasing distance  
 277 from the equator. Zonal asymmetry in  $\tau_{mod}$  is also quite apparent, both due to signif-  
 278 icantly smaller  $\tau_{mod}$  over land vs ocean and zonal variability over just ocean as well. Re-  
 279 gions of larger  $\tau_{mod}$  occur in regions with small nudging tendencies and at low latitudes.

280 The heuristic analysis above suggested that if  $\tau_{mod}$  is significantly smaller than  $\tau_{ndg}$ ,  
 281 or proportional to  $\tau_{ndg}$ , then the time-averaged nudging tendencies could be expected  
 282 to be proportional to  $\tau_{ndg}^{-1}$ . Over the Southern Ocean where additional drag is being ex-  
 283 erted in all nudging runs, both seem to be true to an extent. The  $\tau_{mod}$  estimates increase  
 284 with increasing  $\tau_{ndg}$ , but less so than expected if  $\tau_{mod}$  were truly proportional to  $\tau_{ndg}$ .  
 285 This is perhaps better seen in the maps of  $\tau_{mod}/\tau_{ndg}$  in Fig. 8e-f. The ratio  $\tau_{mod}/\tau_{ndg}$   
 286 decreases as  $\tau_{ndg}$  is increased from about 1/2 when  $\tau_{ndg} = 3$  hrs to about 1/3 when  $\tau_{ndg} =$   
 287 24 hrs.

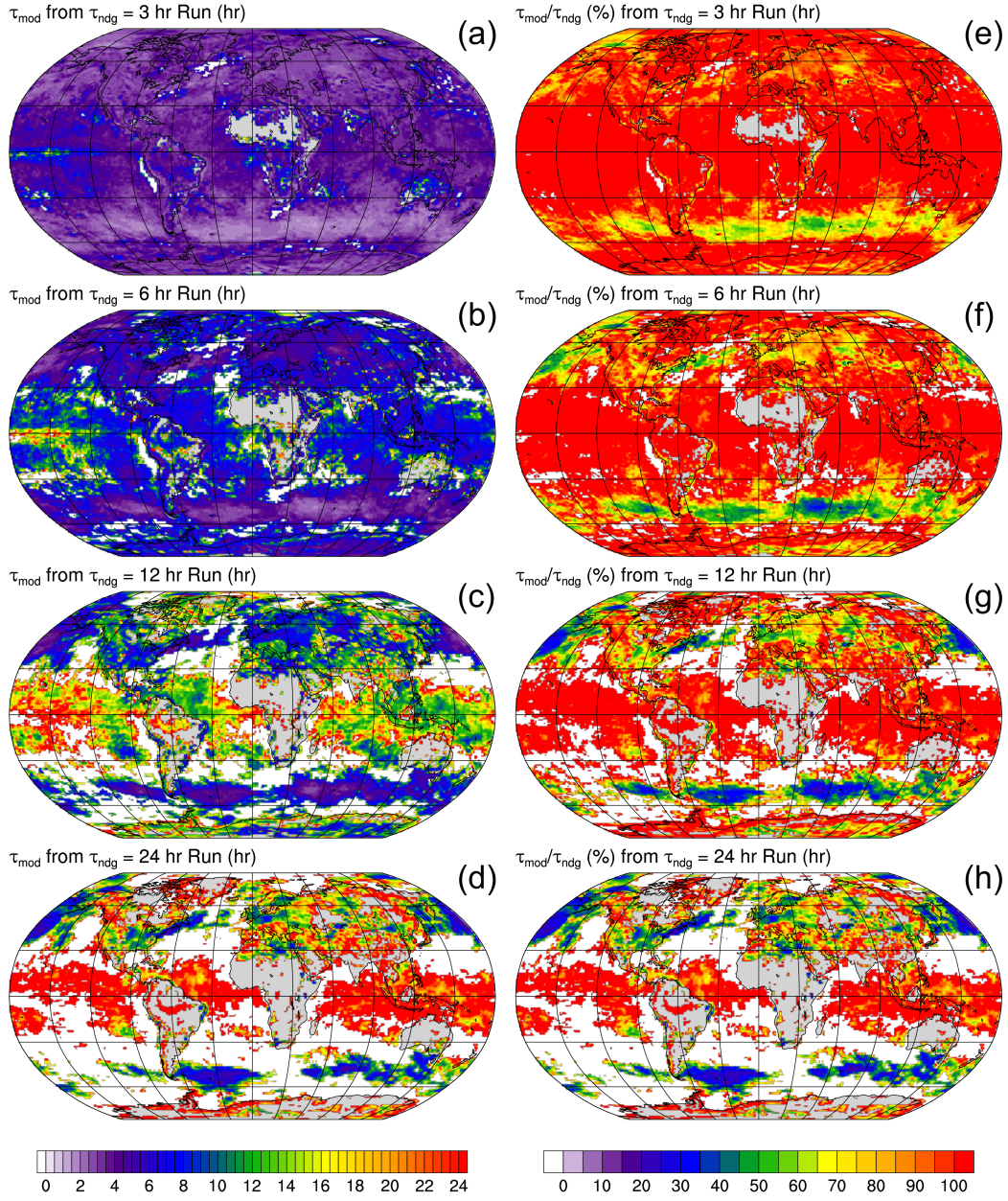


**Figure 8.** Maps of  $\tau_{mod}$  estimated by regressing 3-hr-average  $D_x + P_x$  vs  $u - u_0$  during the 2008-2009 DJF at each grid point on the fourth model level. Both (left)  $\tau_m$  [hr] and (right)  $\tau_m/\tau_n$  [%] are shown. Only regions where the regression slope is statistically significant at the 99% confidence level are shown.

288 All this is to say that the model is quite effective at opposing nudging tendencies,  
 289 in part because the model (the dynamical core in particular) can adjust significantly faster  
 290 (50%-70%) than the nudging term can pull the nudged model state toward the target  
 291 state. Interestingly, the model's adjustment time scales also appear to be dictated, to  
 292 some extent, by the chosen nudging time scale. How the model's dynamical core increas-  
 293 ingly opposes the increasing nudging tendencies is interesting. Perhaps the dynamical  
 294 core makes more efficient use of/uses more adjustment mechanisms/instabilities at its  
 295 disposal to increasingly oppose nudging tendencies' pull away from its desired state. The  
 296 model's response to the nudging tendencies was not investigated further here.

## 297 5 Can Nudging Tendencies Identify Missing/Erroneous Processes?

298 Everything presented thus far was based on CAM simulations with the same con-  
 299 figuration, but with nudging time scales varied. However, a more practical use of the nudg-  
 300 ing method might be to change the model configuration (e.g. parameterizations), per-  
 301 haps as part of a model development or tuning process, and use the nudging tendencies  
 302 to evaluate whether or not the fast model processes have been improved. While it's clear  
 303 nudging tendencies cannot be *quantitatively* interpreted as the net forcing error of the  
 304 model or all its parameterizations because these tendencies depend strongly on the cho-  
 305 sen nudging time scale, nudging tendencies can still point out problem regions qualita-  
 306 tively. Here, nudging tendencies from two CAM runs, one with the Beljaars low-level oro-  
 307 graphic drag parameterization and one without, nudged to ERA5 are briefly compared.  
 308 This parameterization was chosen as it exerts very strong forces on the low-level flow and  
 309 has an easily recognisable spatial distribution (i.e. it mainly acts over significant moun-  
 310 tain ranges).

311 Figure 9 shows the absolute value of changes in DJF-2008-2012-averaged nudging,  
 312 Beljaars, dynamics, and physics tendencies between the two runs. Encouragingly, when  
 313 this parameterization is removed, nudging tendencies act to replace these parameterized  
 314 tendencies (cf. Figs. 9a and b). However, the low-level drag added by the nudging to re-  
 315 place this process is only  $\approx 25\%$  of the tendencies by this process in the run with it en-  
 316 abled. This result further suggests, while nudging tendencies can be useful in identifying  
 317 model errors and/or missing processes, they can only be used qualitatively.

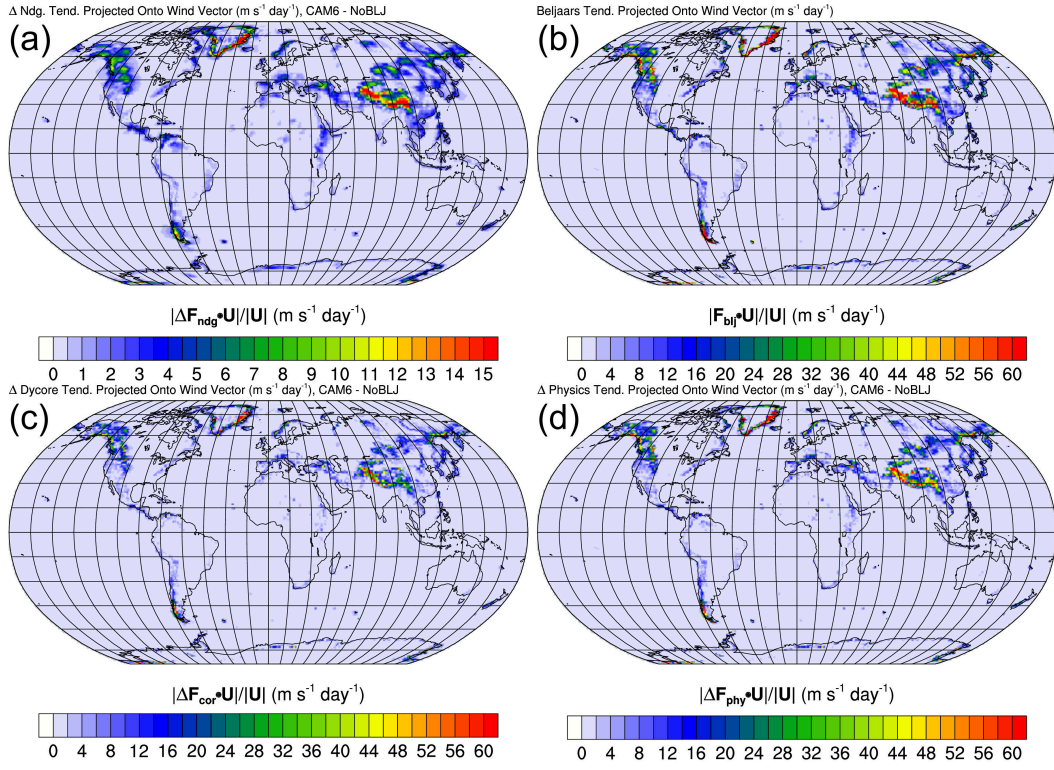


**Figure 9.** Absolute changes in zonal wind tendencies between runs with (CAM6) and without (NoBLJ) the Beljaars turbulent orographic form drag parameterization vertically averaged over the four lowest model levels. (a) Change in zonal wind nudging tendencies. (b) The Beljaars drag tendency. (c) The change in zonal wind dynamics tendencies. (d) The change in the total physics tendency.

## 6 Summary

The primary result of this article is that nudging tendencies that result from nudging a model to a target state are proportional to the inverse of the nudging time scale chosen (Figs. 2, 3a-c). As momentum nudging tendencies increase, they are increasingly compensated by changes in tendencies by the dynamical core (Fig. 7, top row), presumably to adjust to imbalances introduced by the nudging. A heuristic time scale analysis suggests that if the model’s imbalance adjustment time scale is significantly smaller than, or proportional to, the chosen nudging time scales, this result should be expected as long as the target state to which the model is being nudged is different from the state the model is trying to achieve, regardless of the type of target state (e.g. a native analysis, a non-native analysis, some other model entirely that has not assimilated data). The results presented here suggest a model’s imbalance adjustment time scale might be both smaller than, and proportional to, the chosen nudging time scale (Fig. 8).

The consequence of this result is quite important. If nudging tendencies were to be interpreted as total model or physics errors, then the errors so inferred would depend on the nudging time scale chosen. Still, systematic nudging tendencies represent a tendency of the model to push its state away from the target state. If the target state is considered “correct,” then these tendencies still contain some information on model error, even if only qualitatively. However, nudging tendencies cannot be used to, for example, quantitatively identify forcing error profiles by a single parameterization known to dominate forcing in a particular profile.

The relevance of this result is significant as well. Nudging is a ubiquitous capability of numerical weather and climate models and is used widely in a variety of applications. While few have made use of the nudging tendencies themselves, an emerging application is to use methods to predict nudging tendencies of a model given its state in order to improve its predictive skill and reduce long-term biases. Watt-Meyer et al. (2021) and Bretherton et al. (2021) used machine learning to this, with some success, though they differed in the variables nudged and focused on. The results here do not invalidate such results, but suggest that they may depend not only on the model and resolution used, but also on the nudging time scale chosen.

The nudging method of data assimilation and model error quantification is likely the simplest in a spectrum of such methods. The results here are not expected to have any relevance to the initial tendency method or increment tendency methods of model error quantification (e.g. Klinker and Sardeshmukh (1992); Rodwell and Palmer (2007); Cavallo et al. (2016)). However, there may be some relevance to the incremental analysis update (IAU) method (Bloom et al., 1996; Rienecker et al., 2011), which applies analysis increment tendencies, held constant over an analysis window (e.g. 6 hours), in governing equations to “guide” a model’s state along an analyzed trajectory. While there are similarities between the IAU and nudging methods, it is unclear at this point if a similar dependence of analysis increment tendencies on the analysis window chosen might exist.

### Acknowledgments

All authors were supported either by the National Center for Atmospheric Research, which is a major facility sponsored by the National Science Foundation under Cooperative Agreement No. 1852977 or by a Climate Process Team grant from the National Science Foundation (NSF Grant Number(s) AGS-1916689). Simulations were performed with high-performance computing support from Cheyenne (doi:10.5065/D6RX99HX) provided by NCAR’s Computational and Information Systems Laboratory, sponsored by the National Science Foundation. We also wanted to acknowledge interesting and helpful discussions with Judith Berner and Riwal Plougenven during the preparation of this manuscript.

## References

- 368  
369 Anthes, R. A. (1974). Data assimilation and initialization of hurricane prediction  
370 models. *Journal of Atmospheric Sciences*, *31*(3), 702 - 719. doi: 10.1175/1520-  
371 -0469(1974)031<0702:DAAIOH>2.0.CO;2
- 372 Bao, J.-W., & Errico, R. M. (1997). An adjoint examination of a nudging  
373 method for data assimilation. *Monthly Weather Review*, *125*(6), 1355 -  
374 1373. Retrieved from [https://journals.ametsoc.org/view/journals/  
375 mwre/125/6/1520-0493\\_1997\\_125\\_1355\\_aaeoan.2.0.co\\_2.xml](https://journals.ametsoc.org/view/journals/mwre/125/6/1520-0493_1997_125_1355_aaeoan.2.0.co_2.xml) doi:  
376 10.1175/1520-0493(1997)125<1355:AAEOAN>2.0.CO;2
- 377 Bloom, S. C., Takacs, L. L., da Silva, A. M., & Ledvina, D. (1996). Data as-  
378 simulation using incremental analysis updates. *Monthly Weather Review*,  
379 *124*(6), 1256 - 1271. Retrieved from [https://journals.ametsoc.org/view/  
380 journals/mwre/124/6/1520-0493\\_1996\\_124\\_1256\\_dauiau.2.0.co\\_2.xml](https://journals.ametsoc.org/view/journals/mwre/124/6/1520-0493_1996_124_1256_dauiau.2.0.co_2.xml) doi:  
381 10.1175/1520-0493(1996)124<1256:DAUIAU>2.0.CO;2
- 382 Blumen, W. (1972). Geostrophic adjustment. *Reviews of Geophysics*, *10*(2), 485-  
383 528. Retrieved from [https://agupubs.onlinelibrary.wiley.com/doi/abs/  
384 10.1029/RG010i002p00485](https://agupubs.onlinelibrary.wiley.com/doi/abs/10.1029/RG010i002p00485) doi: <https://doi.org/10.1029/RG010i002p00485>
- 385 Bretherton, C. S., Henn, B., Kwa, A., Brenowitz, N. D., Watt-Meyer, O., McGib-  
386 bon, J., ... Harris, L. (2021). Correcting coarse-grid weather and climate mod-  
387 els by machine learning from global storm-resolving simulations. *Submitted to*  
388 *JAMES*, 39. Retrieved from <https://doi.org/10.1002/essoar.10507879.1>  
389 doi: 10.1002/essoar.10507879.1
- 390 Cavallo, S. M., Berner, J., & Snyder, C. (2016). Diagnosing model errors from  
391 time-averaged tendencies in the weather research and forecasting (wrf) model.  
392 *Monthly Weather Review*, *144*(2), 759 - 779. doi: 10.1175/MWR-D-15-0120.1
- 393 Charney, J., Halem, M., & Jastrow, R. (1969). Use of incomplete historical data  
394 to infer the present state of the atmosphere. *Journal of Atmospheric Sciences*,  
395 *26*(5), 1160 - 1163. Retrieved from [https://journals.ametsoc.org/view/  
396 journals/atsc/26/5/1520-0469\\_1969\\_026\\_1160\\_uoihdt.2.0.co\\_2.xml](https://journals.ametsoc.org/view/journals/atsc/26/5/1520-0469_1969_026_1160_uoihdt.2.0.co_2.xml) doi:  
397 10.1175/1520-0469(1969)026<1160:UOIHDT>2.0.CO;2
- 398 Davies, H. C., & Turner, R. E. (1977). Updating prediction models by dynam-  
399 ical relaxation: an examination of the technique. *Quarterly Journal of the*  
400 *Royal Meteorological Society*, *103*(436), 225-245. doi: [https://doi.org/10.1002/  
401 qj.49710343602](https://doi.org/10.1002/qj.49710343602)
- 402 Davis, N. A., Callaghan, P., Simpson, I. R., & Tilmes, S. (2021). Specified dynamics  
403 scheme impacts on wave-mean flow dynamics, convection, and tracer transport  
404 in cesm2 (waccm6). *Atmospheric Chemistry and Physics Discussions*, *2021*,  
405 1-32. doi: 10.5194/acp-2021-169
- 406 Gettelman, A., Hannay, C., Bacmeister, J. T., Neale, R. B., Pendergrass, A. G.,  
407 Danabasoglu, G., ... Mills, M. J. (2019). High climate sensitivity in the  
408 community earth system model version 2 (cesm2). *Geophysical Research Let-  
409 ters*, *46*(14), 8329-8337. Retrieved from [https://agupubs.onlinelibrary  
410 .wiley.com/doi/abs/10.1029/2019GL083978](https://agupubs.onlinelibrary.wiley.com/doi/abs/10.1029/2019GL083978) doi: [https://doi.org/10.1029/  
411 2019GL083978](https://doi.org/10.1029/2019GL083978)
- 412 Hersbach, H., Bell, B., Berrisford, P., Hirahara, S., Horányi, A., Muñoz-Sabater,  
413 J., ... Thépaut, J.-N. (2020). The era5 global reanalysis. *Quarterly Jour-  
414 nal of the Royal Meteorological Society*, *146*(730), 1999-2049. Retrieved from  
415 <https://rmets.onlinelibrary.wiley.com/doi/abs/10.1002/qj.3803> doi:  
416 <https://doi.org/10.1002/qj.3803>
- 417 Jastrow, R., & Halem, M. (1970). Simulation studies related to garp. *Bul-  
418 letin of the American Meteorological Society*, *51*(6), 490 - 514. Retrieved  
419 from [https://journals.ametsoc.org/view/journals/bams/51/6/  
420 1520-0477-51.6.490.xml](https://journals.ametsoc.org/view/journals/bams/51/6/1520-0477-51.6.490.xml) doi: 10.1175/1520-0477-51.6.490
- 421 Kao, C.-Y. J., & Yamada, T. (1988). Use of the captex data for evaluations of  
422 a long-range transport numerical model with a four-dimensional data as-

- 423 simulation technique. *Monthly Weather Review*, 116(2), 293 - 306. doi:  
 424 10.1175/1520-0493(1988)116<0293:UOTCDF>2.0.CO;2
- 425 Kistler, R. E. (1974). *A study of data assimilation techniques in an autobarotropic*  
 426 *primitive equation channel model* (Unpublished doctoral dissertation). The  
 427 Pennsylvania State University, State College, PA.
- 428 Klinker, E., & Sardeshmukh, P. D. (1992). The diagnosis of mechanical dissipa-  
 429 tion in the atmosphere from large-scale balance requirements. *Journal of At-*  
 430 *mospheric Sciences*, 49(7), 608 - 627. doi: 10.1175/1520-0469(1992)049<0608:  
 431 *TDOMDI

432 Mapes, B. E., & Bacmeister, J. T. (2012). Diagnosis of tropical biases and the mjo  
 433 from patterns in the merra analysis tendency fields. *Journal of Climate*,  
 434 25(18), 6202 - 6214. Retrieved from [https://journals.ametsoc.org/](https://journals.ametsoc.org/view/journals/clim/25/18/jcli-d-11-00424.1.xml)  
 435 [view/journals/clim/25/18/jcli-d-11-00424.1.xml](https://journals/clim/25/18/jcli-d-11-00424.1.xml) doi: 10.1175/  
 436 JCLI-D-11-00424.1

437 Plougonven, R., & Zhang, F. (2014). Internal gravity waves from atmospheric jets  
 438 and fronts. *Reviews of Geophysics*, 52(1), 33-76. Retrieved from [https://](https://agupubs.onlinelibrary.wiley.com/doi/abs/10.1002/2012RG000419)  
 439 [agupubs.onlinelibrary.wiley.com/doi/abs/10.1002/2012RG000419](https://doi.org/10.1002/2012RG000419) doi:  
 440 <https://doi.org/10.1002/2012RG000419>

441 Rienecker, M. M., Suarez, M. J., Gelaro, R., Todling, R., Bacmeister, J., Liu, E.,  
 442 ... Woollen, J. (2011). Merra: Nasa's modern-era retrospective analysis  
 443 for research and applications. *Journal of Climate*, 24(14), 3624 - 3648. Re-  
 444 trieved from [https://journals.ametsoc.org/view/journals/clim/24/14/](https://journals.ametsoc.org/view/journals/clim/24/14/jcli-d-11-00015.1.xml)  
 445 [jcli-d-11-00015.1.xml](https://doi.org/10.1175/JCLI-D-11-00015.1) doi: 10.1175/JCLI-D-11-00015.1

446 Rodwell, M. J., & Palmer, T. N. (2007). Using numerical weather prediction to  
 447 assess climate models. *Quarterly Journal of the Royal Meteorological Society*,  
 448 133(622), 129-146. doi: <https://doi.org/10.1002/qj.23>

449 Skamarock, W. C., Klemp, J. B., Dudhia, J., Gill, D. O., Barker, D. M., Duda,  
 450 M. G., ... Powers, J. G. (2008). *A description of the Advanced Research WRF*  
 451 *version 3* (Tech. Rep.). Boulder, Colorado: NCAR Tech. Note NCAR/TN-  
 452 475+STR.

453 Stauffer, D. R., & Seaman, N. L. (1990). Use of four-dimensional data as-  
 454 simulation in a limited-area mesoscale model. part i: Experiments with  
 455 synoptic-scale data. *Monthly Weather Review*, 118(6), 1250 - 1277. doi:  
 456 10.1175/1520-0493(1990)118<1250:UOFDDA>2.0.CO;2

457 Watt-Meyer, O., Brenowitz, N. D., Clark, S. K., Henn, B., Kwa, A., McGibbon,  
 458 J., ... Bretherton, C. S. (2021). Correcting weather and climate models by  
 459 machine learning nudged historical simulations. *Geophysical Research Letters*,  
 460 48(15). Retrieved from [https://agupubs.onlinelibrary.wiley.com/doi/](https://agupubs.onlinelibrary.wiley.com/doi/abs/10.1029/2021GL092555)  
 461 [abs/10.1029/2021GL092555](https://doi.org/10.1029/2021GL092555) doi: <https://doi.org/10.1029/2021GL092555>*